remote sensing

MDPI

Article

Environmental Aftermath of the 2019 Stromboli Eruption

Agnese Turchi [1], Federico Di Traglia [1,*], Tania Luti [1], Davide Olori [2], Iacopo Zetti [3] and Riccardo Fanti [1]

1 Dipartimento di Scienze della Terra, Università degli Studi di Firenze, Via La Pira 4, 50121 Firenze, Italy; agnese.turchi@unifi.it (A.T.); tania.luti@unifi.it (T.L.); riccardo.fanti@unifi.it (R.F.)
2 Dipartimento di Sociologia e Diritto dell'Economia, Alma Mater Studiorum-Università di Bologna, Sede Strada Maggiore 45, 40125 Bologna, Italy; davide.olori@unibo.it
3 Dipartimento di Architettura, Università degli Studi di Firenze, Via Micheli 2, 50121 Firenze, Italy; iacopo.zetti@unifi.it
* Correspondence: federico.ditraglia@unifi.it; Tel.: +39-055-275-5981

Received: 25 February 2020; Accepted: 18 March 2020; Published: 19 March 2020

Abstract: This study focuses on the July-August 2019 eruption-induced wildfires at the Stromboli island (Italy). The analysis of land cover (LC) and land use (LU) changes has been crucial to describe the environmental impacts concerning endemic vegetation loss, damages to agricultural heritage, and transformations to landscape patterns. Moreover, a survey was useful to collect eyewitness accounts aimed to define the LU and to obtain detailed information about eruption-induced damages. Detection of burnt areas was based on PLÉIADES-1 and Sentinel-2 satellite imagery, and field surveys. Normalized Burn Ratio (NBR) and Relativized Burn Ratio (RBR) allowed mapping areas impacted by fires. LC and LU classification involved the detection of new classes, following the *environmental units* of landscape, being the result of the intersection between CORINE Land Cover project (CLC) and local *landscape patterns*. The results of multi-temporal comparison show that fire-damaged areas amount to 39% of the total area of the island, mainly affecting agricultural and semi-natural vegetated areas, being composed by endemic Aeolian species and abandoned olive trees that were cultivated by exploiting terraces up to high altitudes. LC and LU analysis has shown the strong correlation between land use management, wildfire severity, and eruption-induced damages on the island.

Keywords: Sentinel-2; PLÉIADES; optical remote sensing; volcano remote sensing; wildfires; wildfire severity; land use; land cover; regional planning; Aeolian Archipelago; Stromboli

1. Introduction

Explosive eruptions can severely disrupt the environment around volcanoes by depositing large volumes of erodible fragmental material or inducing wildfires on vegetated volcano slopes [1]. Explosions-induced wildfires at Stromboli are common phenomena related to the fallout of incandescent material on dry vegetation. Currently, there is only limited documentation of environmental disturbance due to wildfire triggered by volcanic eruptions [2].

In this paper, the environmental impact on the volcanic island of Stromboli (Italy) of the 3 July 2019 and 28 August 2019 strong explosions (locally called Strombolian paroxysms [3]) have been described, in terms of wildfire severity and changes in the land cover (LC) and land use (LU). Collected data comprise high-spatial-resolution (HSR) optical imagery from PLÉIADES-1 satellites, moderate-spatial-resolution (MSR) from Sentinel-2 Multi-Spectral Instruments (MSI), and field surveys. Multi-temporal data allowed mapping the LC and LU at Stromboli before the 2019 eruptions, as well as the areas impacted by wildfires triggered by the explosions. Moreover, accounts from eyewitness have

been collected soon after the second explosion, in order to constrain the nature, timing, and location of eruption impacts. Interviews were also fundamental for (1) reconstructing the LU, especially for the vegetated areas whose use was not clear from satellite images only, and (2) combined with a field survey in the burnt areas, to validate the remote sensing data.

Stromboli (Figure 1), a volcanic island located in the Tyrrhenian Sea off the northern coast of Sicily, provides an outstanding record of volcanic island geomorphological evolution and of ongoing volcanic phenomena with the example of the "Strombolian" types of eruption. The landscape is the result of the interaction between volcanic activity, geomorphological evolution, and traditional land management. The persistent Strombolian activity is characterized by intermittent explosions from three vent areas (NE, SW, and Central) located in a summit crater terrace [4,5]. This activity is often punctuated by lava overflows from the crater terrace, and/or by flank eruptions, with the outpouring of lava flows from lateral vents [6,7], or by stronger explosions [8]. At Stromboli, wildfires with a small extensions have been observed following intermediate intensity explosions between "ordinary" activity and paroxysmal explosions (locally called major explosions [8]), whereas large-scale wildfire have been triggered by paroxysmal explosions (as in 1768, 1879, 1891, 1906, 1916, 1919, 1930, 1936, 1941, 1943, 1944 and 1950; [3]).

On 3 July 2019, Stromboli experienced a Strombolian paroxysm without long-term precursors [9]. In the following months, lava has outpoured from a vent localized in the SW crater area, and sporadically from the NE one. On 28 August 2019, a new paroxysmal explosion occurred, followed by strong volcanic activity, culminating with a lava flow emitted from the SW-Central crater area [9]. Subsequently, the eruptive activity decreased. Coarse-grained tephra (spatter bombs and ballistics blocks) erupted during 3 July 2019 and 28 August 2019 paroxysms have been mainly accumulated on the summit of the island. The 3 July 2019 tephra fallout (lapilli and ash) has impacted the south-western and southern part of the island, including the village of Ginostra; whereas the 28 August 2019 tephra fallout has affected only a small part of the island, being its dispersal axis easterly directed.

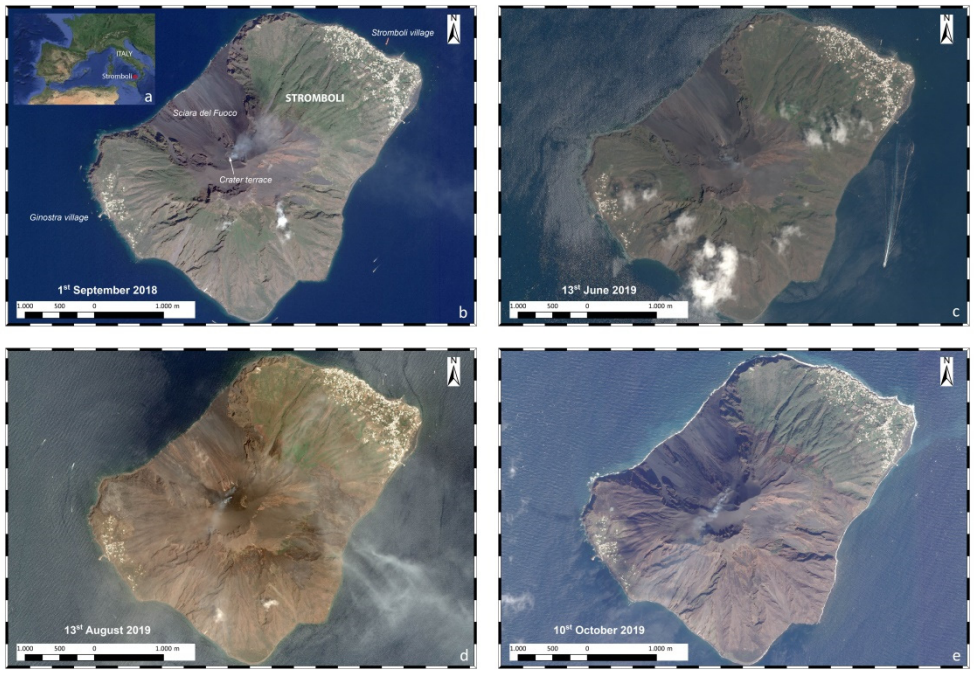

Figure 1. (**a**) Geographic location of the Island of Stromboli (Google Earth image); PLÉIADES-1 images collected on (**b**) 1 September 2018; (**c**) 13 June 2019; (**d**) 13 August 2019; (**e**) 8 October 2019.

2. Materials and Methods

2.1. Wildfire Impact and Severity Recognition

The remote sensing dataset used for the recognition of the impact on the Stromboli environment comprised:

- High-resolution optical images collected by the PLÉIADES (Table 1) constellation (0.5 m × 0.5 m resolution for Panchromatic + 2 m × 2 m Multispectral data) collected on 1 September 2018 (Figure 1b), 13 June 2019 (Figure 1c), 13 August 2019 (Figure 1d), and 8 October 2019 (Figure 1e). Images are 100% cloud free, with a total areal coverage of 58 km^2;
- Multi-temporal Sentinel-2 MSI images (Figure 2), used to constrain the events at higher temporal resolution (Table 2). Sentinel-2 MSI has 13 spectral bands between 0.433 µm and 2.19 µm and pixel resolution between 10 m × 10 m and 60 m × 60 m, depending on the bands. Several band combination and ratio have been used to enhance contrasts between features, as well as to reduce the variations in topographic illumination.

Table 1. Technical characteristics of high-spatial-resolution (HSR) images used for this study.

Acquisition date	**1 September 2018 13 June 2019 13 August 2019 8 October 2019**
Spatial resolution PAN (m)	0.5 × 0.5
Spatial resolution MS (m)	2 × 2
Cloud coverage (%)	<5
Spectral resolution (nm)	
Blue	450–550
Green	490–610
Red	600–720
Near infrared	750–920

The Normalized Burn Ratio (NBR) index has been used to map the areas covered by fire, which has permitted to easily identify the areas covered by the fire and the degree of severity of a fire [10–16]. This index has been calculated on two Sentinel-2 images acquired on different dates before and after the wildfire (after a not excessively high number of days, especially if the area affected by the fire consists mainly of pasture or low bush).

The NBR index has been derived from the following equation:

$$\mathrm{NBR} = \frac{\mathrm{NIR}\ (\mathrm{B8}) - \mathrm{SWIR}\ (\mathrm{B12})}{\mathrm{NIR}\ (\mathrm{B8}) + \mathrm{SWIR}\ (\mathrm{B12})} \quad (1)$$

NIR and SWIR2 are the near infrared and the short wave infrared region reflectance value, respectively. Before a fire, healthy vegetation got very high near infrared reflectance and low infrared reflectance of the electromagnetic spectrum. Recently burned areas have relatively low near infrared reflectance and high reflectance in the short wave infrared band. A high NBR value generally indicates healthy vegetation while a low value indicates that the soil has no plant cover (bare soil) and that the areas have recently been burnt.

The Sentinel-2 images have been pre-processed to obtain reflectance bands, stacked and then a subset containing the island of Stromboli has been selected. For the calculation of the NBR index the Sentinel-2 bands 8 and 12 have been used.

Table 2. Sentinel-2 Multi-Spectral Instruments (MSI) bands.

Band	Description	Wavelength (l)	Resolution (m)
1	*Coastal aerosol*	0.433–0.453	60
2	*Blu*	0.458–0.523	10
3	*Green*	0.543–0.578	10
4	*Red*	0.650–0.680	10
5	*Near InfraRed*	0.698–0.713	20
6	*Near InfraRed*	0.733–0.748	20
7	*Near InfraRed*	0.773–0.793	20
8	*Near InfraRed*	0.785–0.900	10
8A	*Near InfraRed*	0.855–0.875	20
9	*Water vapor*	0.935–0.955	60
10	*ShortWave InfraRed–Cirrus*	1.365–1.385	60
11	*ShortWave InfraRed*	1.565–1.655	20
12	*ShortWave InfraRed*	2.100–2.280	20

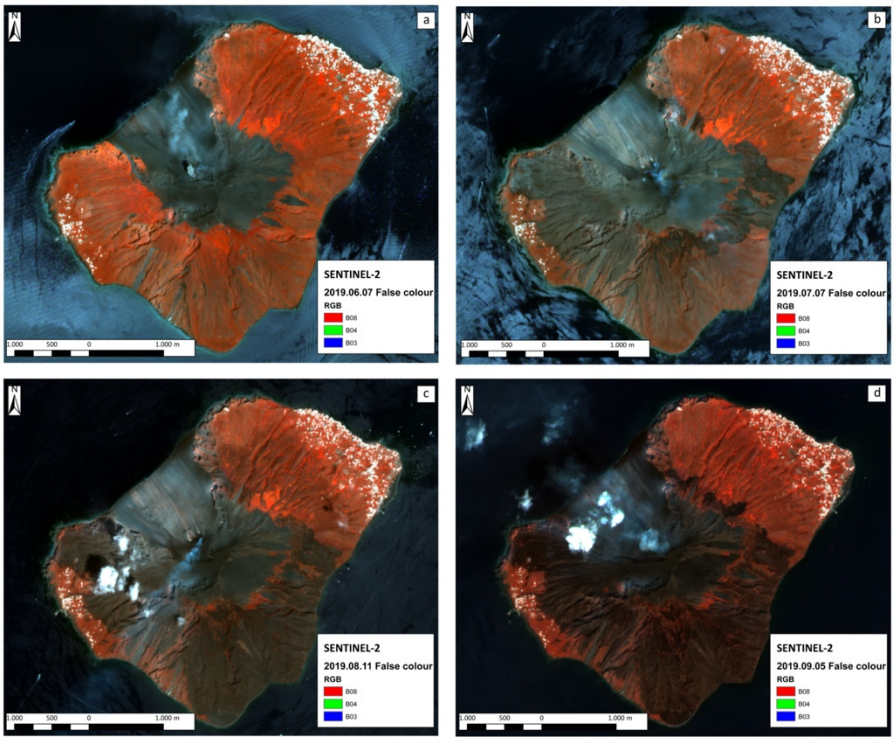

Figure 2. Sentinel-2 image (false color) collected on: (**a**) 7 June 2019 (pre-eruption), (**b**) 7 July 2019, (**c**) 11 August 2019, (**d**) 5 September 2019.

The band 12 has a spatial resolution of 20 m, therefore this image has been resampled at 10 m to conform it to the spatial resolution of the other bands, which as specified above, has spatial resolutions ranging from 10 m to 60 m.

Processing phases can be summarized as follow (Figure 3):

- Data searching and downloading;
- Image pre-processing, through calibration, resampling, stacking, and subsets creation;

- Bands extraction;
- Index calculation: NBR, Normalized Difference Vegetation Index (NDVI), and Relativized Burn Ratio (RBR) [12], obtained as the difference between the NBR index of the images acquired before and after the event;
- Classification of the severity of the event, by converting the values of the indices into severity levels;
- Definition of the area covered by the wildfires.

RBR has been calculated using the following equation:

$$\mathrm{RBR} = \frac{\mathrm{dNBR}}{\mathrm{NBRpre} + 1,001} \tag{2}$$

where:

$$\mathrm{dNBR} = \mathrm{NBR_{pre}} - \mathrm{NBR_{post}} \tag{3}$$

and where $\mathrm{NBR_{pre}}$ e $\mathrm{NBR_{post}}$ are referred to the index calculated on the image before and after the wildfire, respectively. The dNBR is an absolute difference that can present a problem in areas with low vegetation cover as the absolute value of NBR before and after the event may be very small (Figure 4). In such situations, the value of the RBR index provides better results.

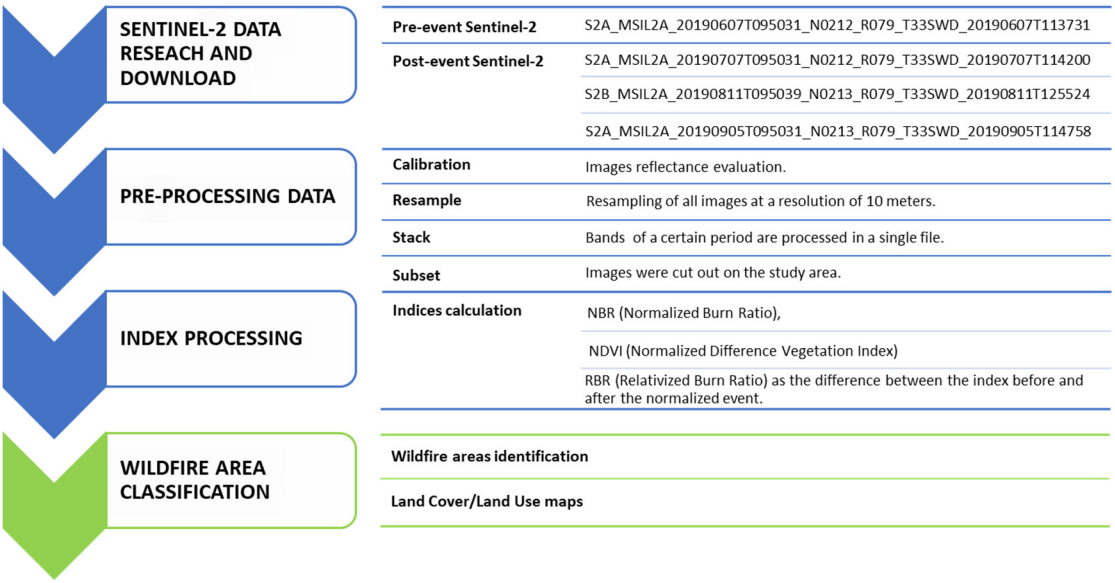

Figure 3. Flowchart summarizes the image processing procedure for the wildfire impact and severity mapping.

The RBR values have been used to derive the map of the areas impacted by the wildfire produced by the 2019 paroxysmal explosions. The USGS FireMon program, a National Burn Severity Mapping Project of the U.S. Geological Survey, indicates severity layer variable [16]. The calculated values usually vary because of the different characteristics of the image and the acquisition conditions; in the case of Stromboli, all areas with an RBR value greater than 0.270 have been considered burnt areas. In our case we used the thresholds proposed by the USGS to distinguish the areas covered by the fire from the not burned areas, not to define the severity. PLÉIADES optical images, field inspections, and eyewitness accounts have been used to validate the results.

2.2. Multi-temporal Land Cover and Land Use Analysis

PLÉIADES-1 optical imagery collected before (1 September 2018, 13 June 2019), during (13 August 2019), and following the 2019 eruption (8 October 2019) have been used to constrain the LC and LU changes. Although the terms LC and LU are often used as synonyms, they have different meanings:

on the one hand, the LC is defined as the type of coverage of anthropic and non-anthropic surfaces, characterized by different degrees of ecological complexity; on the other hand the LU is referred to the type of management/use of soil resources, in relation to the peculiarities of the local socio-economic system [17].

Multi-temporal comparison of LC and LU has been based on the digitalization of images collected before and after the eruption. The dataset comprised also Panchromatic and Multispectral Very High Resolution (VHR) optical imagery with spatial resolution of 0.5 and 2 m, respectively (see ref. [18]). To assess the accuracy of the horizontal position in the PLÉIADES-1 images, Ground-Control Points (GCPs) were collected on the map database (Cartographic XY standard deviation: 0.15 m). A block adjustment including all the satellite scenes was performed. The block adjustment was validated when the following accuracy was achieved: (i) pixel xy bias smaller than 0.3 pixels; (ii) pixel xy standard deviation smaller than 0.3 pixels; (iii) pixel xy maximum smaller than 2 pixels. Comparison has involved the definition of new LC and LU classes whose details have been calibrated on different reduction scales from 1:2.000 to 1:10.000, following the environmental units that made up the Stromboli landscape. Classes have been derived from the III level classes of the CORINE Land Cover project (CLC) and to IV level classes of the *Cartografia tematica Uso del Suolo* project (topographical Tuscany Region DATABASE) made by LaMMA Consortium. At the same time, new classes have been introduced considering local landscape patterns (Table 3). The different areas identified for the LC and LU were manually segmented. As far as the burned areas are concerned, the data deriving from the RBR were used, manually segmented, and validated by PLÉIADES-1 image analysis. This validation was strengthened by field surveys and eyewitness accounts.

Table 3. Land cover (LC) and land use (LU) classes.

LAND COVER	LAND USE
Artificial areas	Buildings
	Adjacent areas
	Infrastructures
	Urban green areas
	Sport facilities
	Industrial areas, public services, power stations
	Airports, helipads, harbors
	Landfills
	Cemeteries
	Archaeological areas
Agricultural areas	Vineyards
	Mixed agricultural woody crops (olive groves, citrus groves)
	Ancient olive groves, shrubberies and Mediterranean bushes
Semi-natural vegetated areas	Uncultivated areas
	Shrubberies and Mediterranean bushes
	Herbaceous and shrub vegetation evolving
Semi-natural not vegetated areas	Cliffs and rocks with poor or absent vegetation
	Lava and lapilli fields
	Dunes, sands
	Artificial rocks
Fire-damaged areas	Fire-damaged areas

Furthermore, linear (contour lines, drainage network, infrastructure, dividing elements) and polygonal (buildings) elements of ATA Regional Technical Map (edition 2012-2013) and ground morphology from PLÉIADES tri-stereo Digital Elevation Model (collected on 1 September 2018; see [18] for DEM details) have been used to define every single "patch," to scale 1:2.000. In addition to the evaluation of abundance of each class in 2018 and 2019, the percentage variation of land cover and use has been calculated to estimate the degree of loss, following recent eruptions (Appendix A).

2.3. Social Analysis

The eyewitnesses accounts have been crucial to validate LC and LU analysis results (to shift from the LC to LU), and to obtain more detailed information in terms of nature, timing and location of post-eruption damages [19]. Semi-structured interviews have been initially designed to assess the risk perception of whom usually lives on the island of Stromboli, for more than six month per year. The interviews have been collected between 29 August and 7 September 2019; although the paroxysms have influenced the outcome of social research.

A sample of 20 eyewitnesses, between 24 and 76 years old, from Stromboli and Ginostra villages have been chosen, in order to collect different data from geographically separated places, affected by the same paroxysmal explosions.

Social research has concerned (Appendix B, Appendix C):

- To validate LC and LU analysis results;
- Reconstruction of the events;
- Perception of 3 July and 28 August 2019 paroxysms, from Stromboli and Ginostra villages;
- Damages assessment to the urbanized and non-urbanized areas (agricultural and semi-natural lands), following each explosion.

The interviews have been conducted orally, within a time period between 10 and 50 minutes; the use of recorders and transcriptions has allowed not to lose data. The attention has mainly focused on the witnesses' account, separating the information found in Stromboli village from that found in Ginostra village, in relation to the first and the second paroxysm.

3. Results

3.1. LC/LU Evolution

Sentinel-2 data images and derived maps have allowed a dense temporal scan of the burned areas and the progression of the fires on the vegetated area. On the entire island of Stromboli, Sentinel-2 images were acquired every 10 days. However, only a part of these images were used for this study because of high local cloud cover (Figure 4). For this reason, the integration between the results of the satellite data and the interviews with the eyewitnesses, allowed to define well all the phenomena that have contributed to damage the vegetation.

The 3 July 2019 explosion produced most of the wildfires that started immediately, as soon as the tephra have begun to fall. A second fire broke out on 25 July 2019, but it was related to the incomplete reclamation of the burned areas on 3 July 2019. Contrariwise, the 28 August 2019 explosion did not produce significant wildfires, except of a small area in the northern part of the island (Figures 4 and 5). At the end of the eruption, wildfires burnt 4,964,741.8 m^2, equal to 39.35% of the total area of the island (Figures 6 and 7).

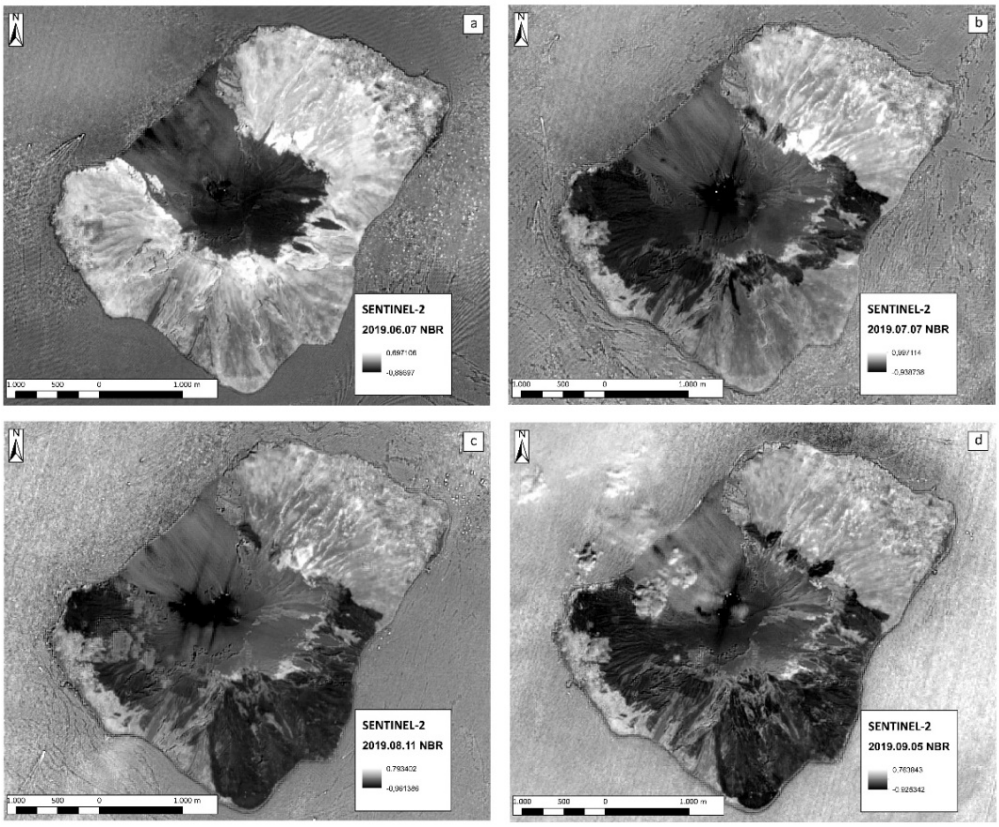

Figure 4. Sentinel-2 images-derived NBR on: (**a**) 7 June 2019 (pre-eruption), (**b**) 7 July 2019, (**c**) 11 August 2019, (**d**) 5 September 2019. Thermal (black) anomalies in the summit area and Sciara del Fuoco in (**b**), and (**c**), are related to the effusive activity.

It is important to remark that *Artificial areas* were not particularly impacted, except for *Industrial areas, public services, and power station* that decreased by 14.10%. During field surveys, most of the damages were detected near photovoltaic power station in Ginostra village. Instead *Adjacent areas* (including vegetable gardens, gardens, paved surfaces of different permeability) suffered a small decrease (0.50%).

Agricultural areas (characterized by Ancient olive groves, shrubberies and Mediterranean bushes) or Semi-natural vegetated areas (characterized by only Shrubberies and Mediterranean bushes) in 2018 and 2019 decreased by 34.20% and 81.10%, respectively. Today the second one represent 6.82% (860,617.4 m^2) of the total area of the island, compared to 2018 in which it represented 36.15% (4,561,225.8 m^2). The agricultural productive areas, characterized by mixed agricultural woody crops (olive groves and citrus groves) and organized in promiscuous crops, represent 1.60% (202,151.5 m^2) of total area and decreased by 9.40%.

Finally, the 3 July 2019 paroxysm also caused loss of vegetation corresponding to *Uncultivated areas* and *Cliffs and rocks with poor or absent vegetation* that decreased by 0.9% and 32.9%, respectively.

The interpretation process of land cover and use was particularly difficult in correspondence of urbanizations and agricultural areas characterized by wild terraced olive groves, shrubbery, and bushes. In the first case the peculiarities of Aeolian buildings (i.e., square shapes, planimetric development of structures, large terraced areas, outdoor porch spaces) [20] and the complex organization of interior spaces of the houses did not facilitate the identification of vegetable gardens. It was necessary to combine all patches near the buildings to single class. In the second case it was not possible to clearly define the limit of patches where abandoned olive groves characterized by re-naturalized areas were adjacent to shrubberies and Mediterranean bushes. Therefore, not only the ground arrangement of olive trees and the foliage but also terraces along the slope were considered as main indicators.

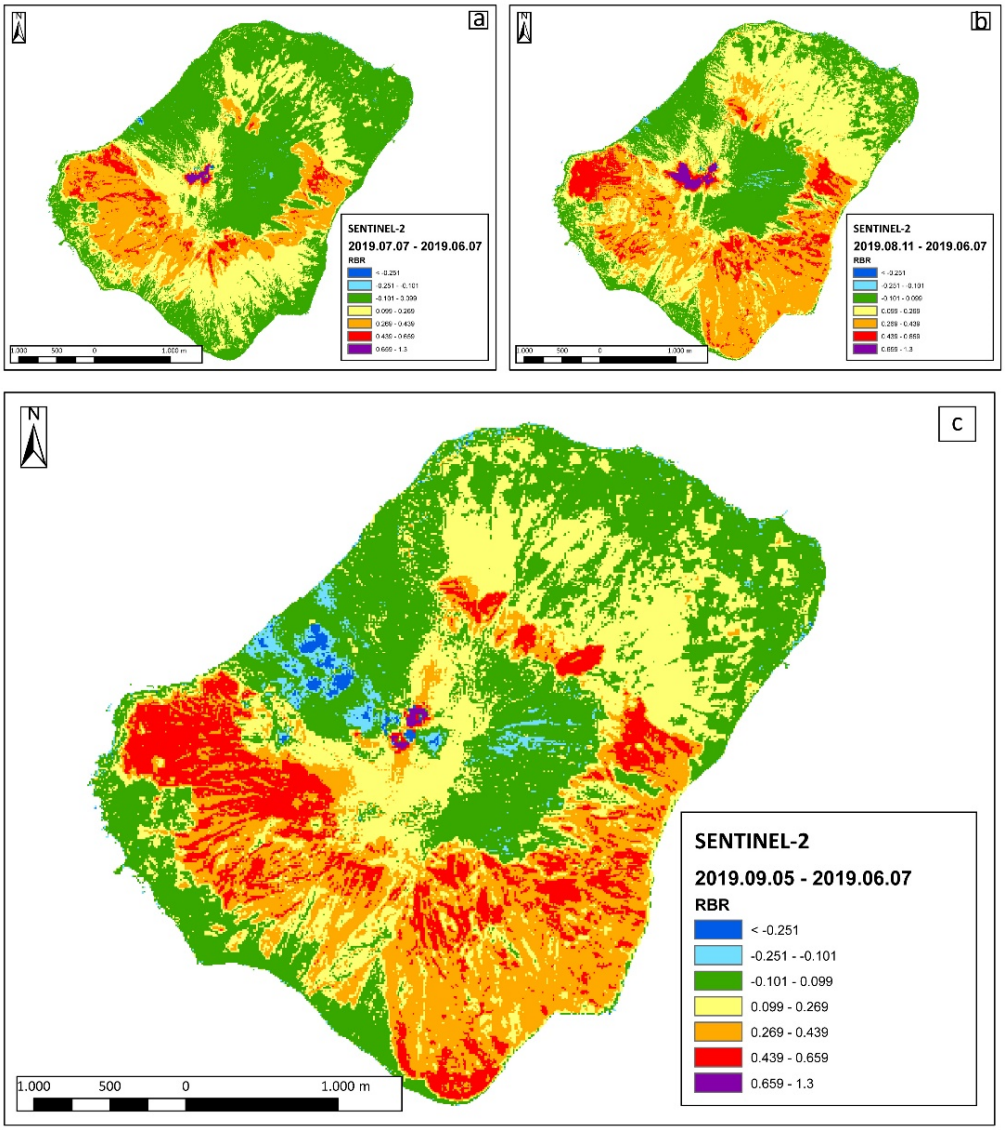

Figure 5. Sentinel-2 images-derived Relativized Burn Ratio (RBR) on: (**a**) 7 June 2019–7 July 2019, (**b**) 7 June 2019–11 August 2019, (**c**) 7 June 2019–5 September 2019.

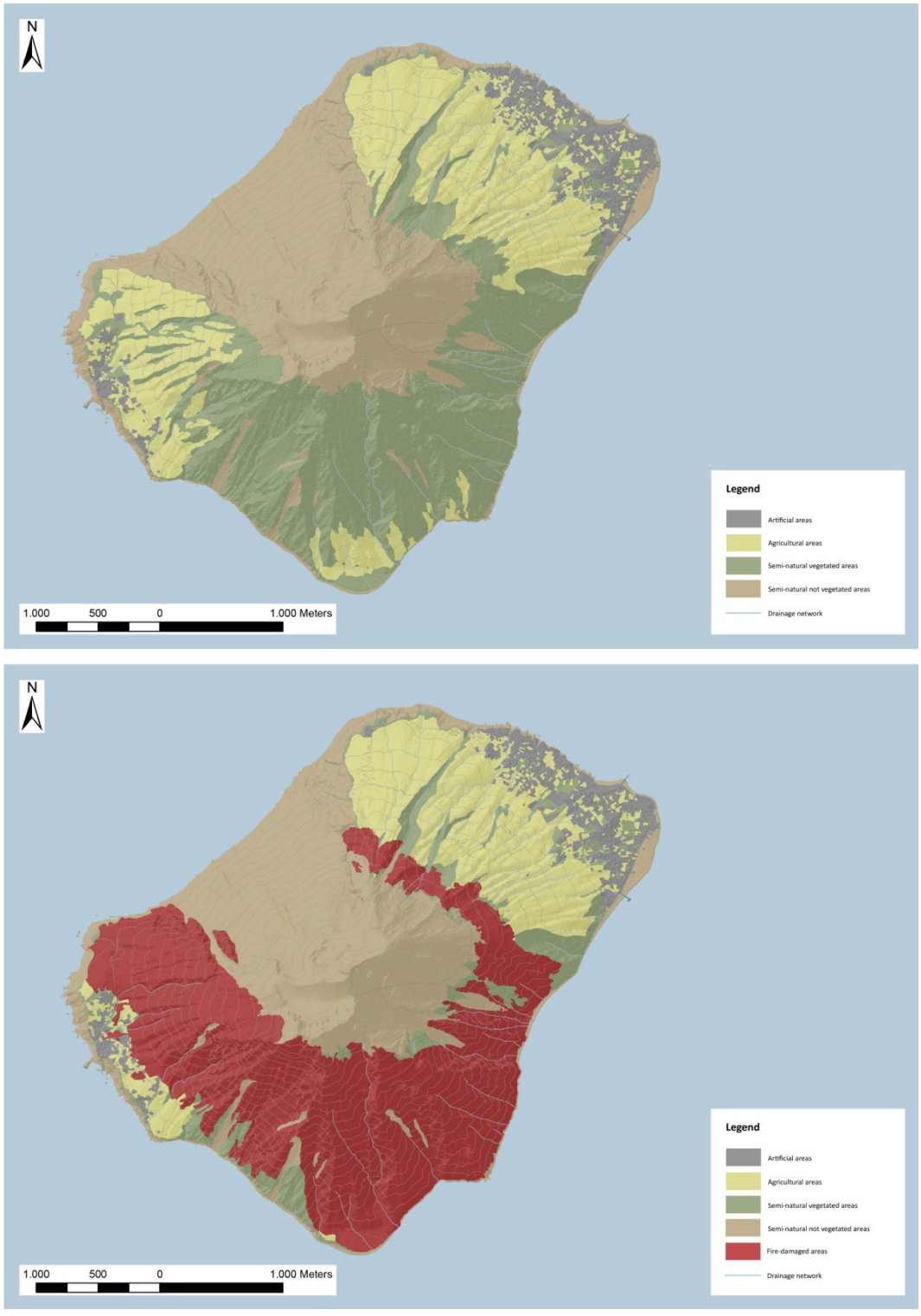

Figure 6. Land cover map (LC) pre-eruption (2018) and post-eruption (2019).

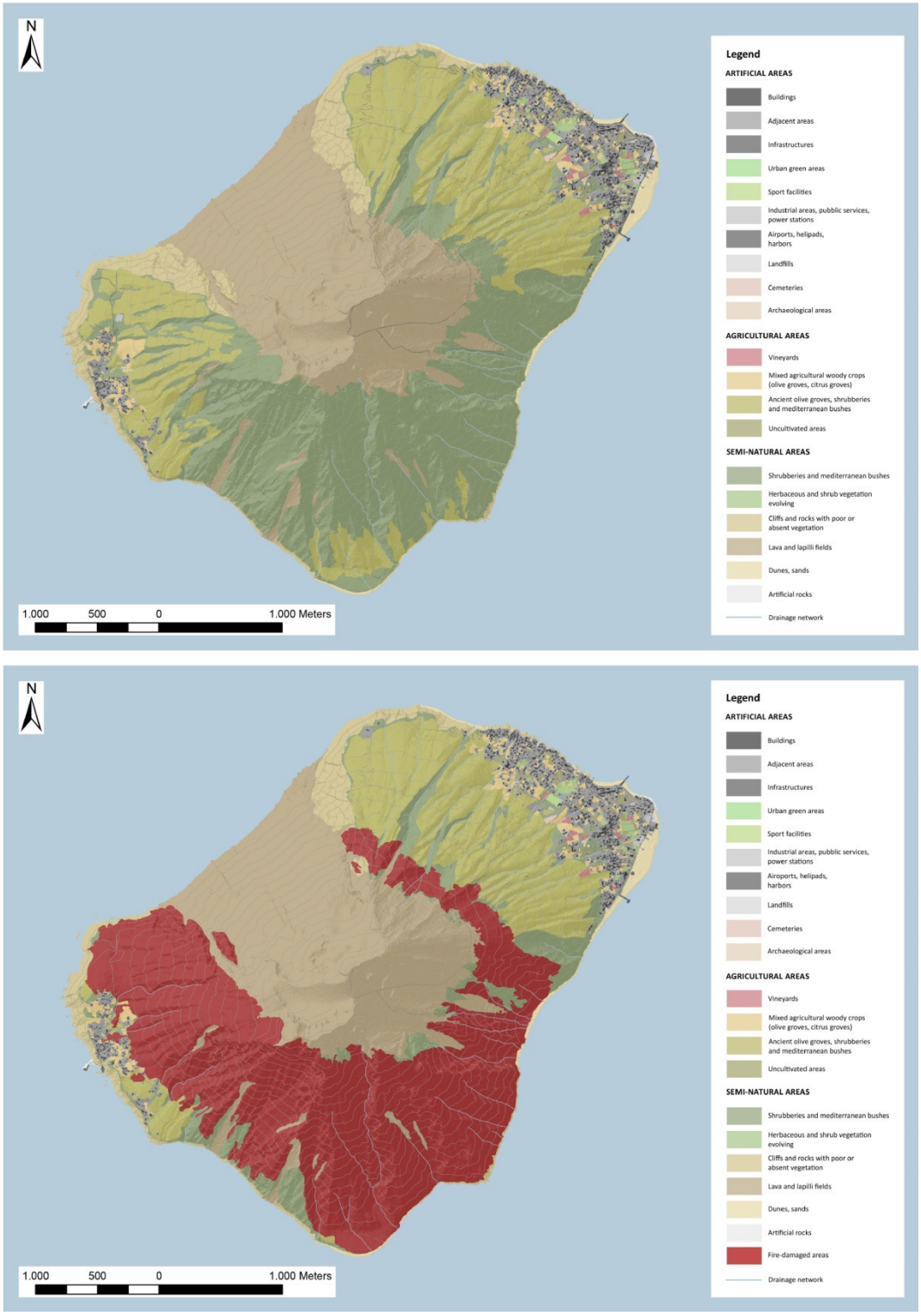

Figure 7. Land use map (LU) pre-eruption (2018) and post-eruption (2019).

3.2. *Eyewitnesses Accounts*

According to the results obtained from the analysis of satellite images, all witnesses observed low damages to the urbanized areas. People saw ash accumulation on the roofs, being afraid of the obstruction of rainwater harvesting cisterns (Appendix B, Appendix C). As reported by the Interviewees n. 10, 18, 19, and 20, some properties suffered damages to canopies and photovoltaic panels placed on

the roofs (Figure 8), following tephra fallout in Ginostra; near Punta Corvi (the south-western edge of the Sciara del Fuoco), the adjacent area of the photovoltaic power station was completely burnt by fire (Figure 9). Most of the witnesses saw significant damages to the not-urbanized areas, without providing specific details about the LC and LU typologies that were impacted (Figure 10).

The results of interviews have been summarized in Appendices B and C. The first event, which mainly affected Ginostra, was perceived particularly violent; the Interviewee n. 20, as well as n. 18, defined the paroxysm "[...] a very different and more devastating explosion" than the previous ones. The second event, which mainly affected Stromboli, was also described in detail by those who reside there and the perception was of a strong but not destructive event like the first one. The surroundings of Ginostra seems to be the most affected area by the 3 July 2019 paroxysm; according to the Interviewees n. 18 and 19, fire has licked up the properties without affecting masonry structures. It was possibly because of the regular maintenance of private gardens, unlike terraced olive groves that are still abandoned. According to the Interviewees n. 1, 13, 14, and 17, Stromboli was affected also by the paroxysm of 28 August 2019 and in this case, the fire was far enough from the buildings. All the witnesses mentioned the casualty near Punta Corvi, in consequence of the event of 3 July 2019; the great deal of media attention certainly enhanced the general perception of damages.

Figure 8. Tephra accumulation on the roofs in (**a**,**b**), damages to the canopies in (**c**,**d**) at Ginostra, following the 3 July 2019 paroxysmal explosion.

The social research, based on semi-structured interviews, found some difficulties. The main one was finding available witnesses to release testimonies; the occurrence of two close paroxysmal explosions, the restrictions imposed by civil protection authorities on access to the island and volcano, the tourism decrease, and media echo generated people discontent and stress. Fortunately, it was possible to collect interviews because of the trustful relationship established in the previous months.

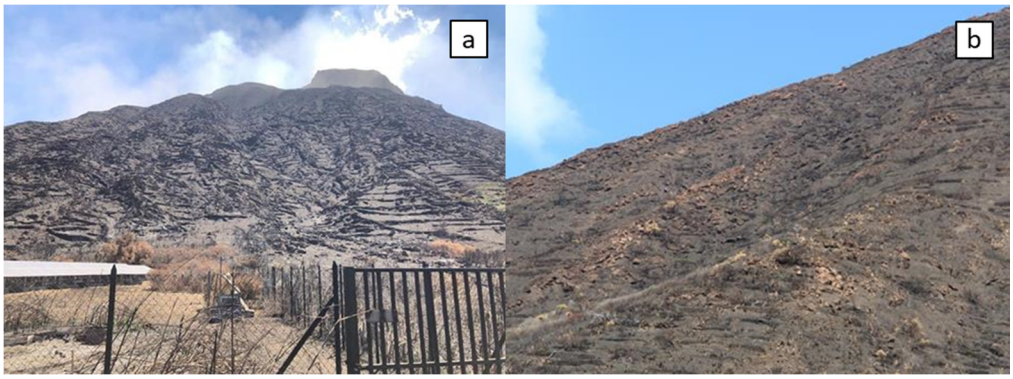

Figure 9. Damages to the adjacent area of the photovoltaic power station in (**a**), damages to the ancient terraced olive groves in (**b**) at Ginostra, following the 3 July 2019 paroxysmal explosion.

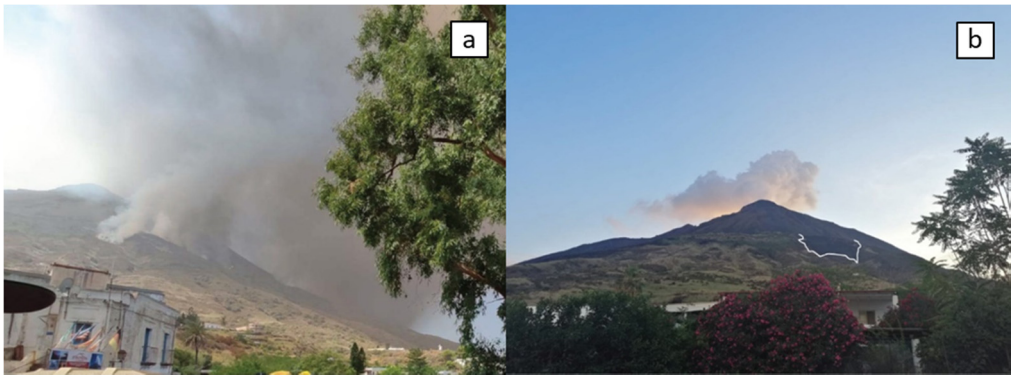

Figure 10. (**a**) wildfire near Stromboli village and (**b**) fire damages, following the 28 August 2019 paroxysmal explosion.

4. Discussion

Explosive eruptions can severely disrupt the environment around volcanoes by depositing large volumes of erodible fragmental material, altering boundary conditions of fluvial systems increasing erosion rate and drainage mass flux (water and sediment) in the affected basin [21–27]. However, low to moderate intensity eruptions have a modest impact on the surrounding environment, unless there are settlements very close to the emission vents (i.e., ref [28] and ref [29]). This is true if secondary effects are not considered. In the case of Stromboli, the phenomenon considered most dangerous is specifically a secondary event, i.e., the eruption-induced tsunamis (triggered by landslides or pyroclastic density currents) [8]. On the other side, for the (major or paroxysmal) explosions, primary hazards have always been associated with phenomena such as ballistics [30] and hot rock avalanches [31]. However, volcanic activity can eject centimeter-sized incandescent bombs/blocks up to some kilometers away from the vent, and each clast can eject in turn incandescent fragments from the impact site, stirring up wildfires on vegetated areas [8].

The 3 July 2019 explosion demonstrate that a moderate intensity explosion has impacted severely on the island, causing a casualty and inducing a wide-spread wildfire. While the causes of the death are unclear, the causes of the vastness of fires are due to natural (the explosion produced many ballistic projectiles and lapilli fallouts on dry vegetated areas) and anthropogenic factors like agricultural land abandonment. The research has shown that the most affected areas by wildfires have been those ones characterized by wild terraced olive groves and Mediterranean shrubberies and bushes, with an overproduction of highly flammable fuel indeed. According to the results of semi-quantitative analyses and semi-structured interviews, fire-damaged areas are mainly distributed in the south-western and northern part of the island. To date, a quite large area of the eastern flank

of the volcano, not so far from Stromboli village, still remains vegetated as well as some small areas unevenly distributed in the southern flank, near Ginostra.

Multi-temporal LC and LU analyses have allowed to estimate not only damages in terms of loss of Aeolian endemic vegetation and agricultural heritage [32,33], but also transformations of landscape patterns related to the land management changes [34]. Until 1930s, inhabitants usually cultivated terraces up to 600–700 meters above the sea level with olive groves, vineyards, and capers, traditionally sown in promiscuous crops [20]. Following the 1930 eruption, the depopulation of the island led to agricultural woody crops abandonment and wilderness. Because of sociocultural and economic production system changes, the abandonment process has consequently caused:

- Physical impoverishment of terraces (dry stone walls and access roads poor maintenance);
- Reduction of hydraulic land management, in terms of outflow water drainage;
- Increase of hydrogeological risk factors;
- Reduction of crop diversity;
- Reduction of landscape variety;
- Loss of cultural heritage, in terms of material and immaterial settlings;
- Loss of agricultural knowledges, techniques and practices.

Therefore LC and LU analyses are crucial to define the best strategies and policies that could be adopted to encourage a sustainable site-specific land management [35–40], taking into account the probability of occurrences of wildfires at Stromboli island. Although there are many variables that can influence the wildfires ignition and spread (e.g., topography, weather, ignition sources), however LC and LU are the only ones that may change substantially [34]. In this case, wild terraced olive groves (almost the 15% of the island) are not only potentially productive but could also reduce risk factors related to paroxysmal events, if they are properly managed. Reducing fuel loads through the land clearing and vegetation structure maintenance can considerably decrease the velocity of wildfires ignition and spread [34,41–44].

5. Conclusions

At Stromboli Island substantial transformations of land cover (LC) and land use (LU) have occurred in consequence of the 3 July and 28 August 2019 paroxysmal explosions; a strong decrease of *Agricultural areas* (mainly *Ancient olive groves, shrubberies and Mediterranean bushes*), *Semi-natural vegetated areas* (*Shrubberies and Mediterranean bushes*), and *Artificial areas* (mainly *Industrial areas, public services and power station*).

The comparison between high-spatial-resolution (HSR) optical imagery from PLÉIADES-1 satellites and moderate-spatial-resolution (MSR) from Sentinel-2 Multi-Spectral Instruments (MSI) using NBR, NDVI, and RBR indexes, has been used to easily identify fire-damaged areas and severity of fires. Multi-temporal analysis has allowed the evaluation the degree of loss in terms of percentage variation of LC and LU classes from 2018 (pre-eruption) to 2019 (post-eruption). Eyewitness accounts have been helpful to define nature, timing, and location of the impacts of paroxysmal events.

The study has allowed to assess the environmental aftermath also in terms of socio-cultural, economic, and ecological consequences of two close paroxysms. Anthropogenic factors like agricultural land abandonment and naturalization of terraced woody crops have increased fire hazard due to the overproduction of highly flammable fuel load (plant biomass) and increase in landscape homogeneity. At the same time agricultural heritage and landscape variety have been compromised.

Finally, our study points out the importance of an accurate methodology through:

- The integration of remote sensing analysis with social analysis that has permitted to collect complete and accurate data;
- The use of correct reduction scales and imagery resolution in remote sensing analysis (also considering social surveys, conducted at local scale);

- Semi-structured interviews, that have allowed to evaluate inhabitants perception of paroxysmal events and real damages;
- The link between multi-temporal LC/LU analysis and social analysis, that has permitted to clarify the consequences of agricultural woody crops abandonment and riparian vegetation poor management, in terms of wildfire propagation.

Author Contributions: Conceptualization: A.T., F.D.T.; data analysis: A.T., T.L.; investigation and methodology: D.O.; writing—original draft preparation: A.T., F.D.T.; writing—review and editing: I.Z., R.F. All authors have read and agreed to the published version of the manuscript.

Funding: This work has been financially supported by the "Presidenza del Consiglio dei Ministri–Dipartimento della Protezione Civile" (Presidency of the Council of Ministers–Department of Civil Protection); this publication, however, does not reflect the position and the official policies of the Department.

Acknowledgments: We thank all the UNIFI staff involved in the crisis management. The authors are particularly grateful to Salvatore Zaia for the logistic support during the 2019 Stromboli eruption.

Conflicts of Interest: The authors declare no conflict of interest.

Appendix A

Table A1. Percentage variation of land cover/land use classes pre-eruption, sin- and post-eruption.

Legend Class LAND COVER	Legend Class LAND USE	Pre-Eruption 2019		Post-Eruption 2019		Percentage Variation (%)
		Area m^2	%	Area m^2	%	
Artificial areas	*Buildings*	160,741	1.27	160,741	1.27	0
	Adjacent areas	412,005	3.27	409,919	3.25	−0.5
	Infrastructures	101,009	0.80	101,009	0.80	0
	Urban green areas	1418	0.01	1418	0.01	0
	Sport facilities	5345	0.04	5345	0.04	0
	Industrial areas, public services, power stations	21,883	0.17	18,802	0.15	−14.1
	Airports, helipads, harbors	7341	0.06	7341	0.06	0
	Landfills	1512	0.01	1512	0.01	0
	Cemeteries	5579	0.04	5579	0.04	0
	Archaeological areas	2191	0.02	2191	0.02	0
Agricultural areas	*Vineyards*	21,822	0.17	21,822	0.17	0
	Mixed agricultural woody crops (olive groves, citrus groves)	223,145	1.77	202,151	1.60	−9.4
	Ancient olive groves, shrubberies and Mediterranean bushes	2,875,753	22.79	1,893,250	15.01	−34.2
Semi-natural vegetated areas	*Uncultivated areas*	63,749	0.51	63,182	0.50	−0.9
	Shrubberies and Mediterranean bushes	4,561,225	36.15	860,617	6.82	−81.1
	Herbaceous and shrub vegetation evolving	46,031	0.36	46,031	0.36	0%
Semi-natural not vegetated areas	*Cliffs and rocks with poor or absent vegetation*	774,354	6.14	519,454	4.12	−32.9
	Lava and lapilli fields	3,182,509	25.23	3,182,506	25.23	0
	Dunes, sands	142,661	1.13	142,661	1.13	0
	Artificial rocks	6196	0.05	6196	0.05	0
Fire-damaged areas	*Fire-damaged areas*	0.0	0,00	4,964,742	39.35	–
	Total area	**12,616,477**	**100%**	**12,616,477**	**100%**	**–**

Appendix B

Table A2. Summary of semi-structured interviews to the inhabitants of Stromboli island, after the 3 July 2019 explosion.

3 July 2019 Explosion				
Eyewitnesses	*Age*	*Location*	*Event description*	*Damages description*
1	26	–	–	1 casualty
2	46	Stromboli (San Vincenzo)	(1) Violent explosion, ash column upwards. (2) Ash/lapilli fall at Ginostra.	1 casualty; Wildfires on vegetated areas at Ginostra; Ash/lapilli accumulation on the roofs (obstruction of rainwater harvest cisterns and dirty water) at Ginostra.
3	49	Stromboli (San Vincenzo)	(1) Explosion, ash column upwards.; (2) Pyroclastic flow towards Sciara del Fuoco.	1 casualty
4	≈75	Stromboli (San Vincenzo)	n.d.	1 casualty
5	68	Stromboli (San Vincenzo)	n.d.	Ash/lapilli accumulation on the roofs (obstruction of rainwater harvest cisterns and dirty water) at Ginostra.
6	51	Stromboli (Pizzillo)	(1) Violent explosion, ash column upwards; (2) Lava flows; (3) Ash/lapilli fall at Ginostra.	Ash/lapilli accumulation on the roofs (obstruction of rainwater harvest cisterns and dirty water) at Ginostra.
7	65	Stromboli (at sea)	n.d.	n.d.
8	58	Stromboli (San Vincenzo)	n.d.	1 casualty
9	28	Ginostra (Punta Corvi)	(1) Explosion, ash column upwards; (2) Lava overflows; (3) Tsunami waves; (4) Ash/lapilli fall at Ginostra.	1 casualty; Ash/lapilli accumulation on the roofs (obstruction of rainwater harvest cisterns and dirty water) at Ginostra.
10	46	n.d.	(1) Explosion, ash column upwards; (2) Ash/lapilli fall at Ginostra.	Wildfires on vegetated areas at Stromboli and Ginostra; Ash/lapilli accumulation on the roofs (obstruction of rainwater harvest cisterns and dirty water) at Ginostra; Damages to the adjacent area of the photovoltaic power station at Ginostra.
11	67	–	–	1 casualty
12	60	–	–	1 casualty
13	≈75	Stromboli (Scari)	(1) Violent explosion, ash column upwards; (2) Ash/lapilli fall at Stromboli and Ginostra.	1 casualty; Wildfires on vegetated areas at Stromboli and Ginostra; Ash/lapilli accumulation on the roofs (obstruction of rainwater harvest cisterns and dirty water) at Stromboli and Ginostra.
14	72	n.d.	(1) Violent explosion, ash column upwards; (2) Ash/lapilli fall at Stromboli and Ginostra.	Wildfires on vegetated areas at Ginostra; Ash/lapilli accumulation on the roofs (obstruction of rainwater harvest cisterns and dirty water) at Stromboli and Ginostra.
15	24	Stromboli (Scari)	n.d.	1 casualty; Wildfires on vegetated areas at Ginostra.
16	76	Stromboli (Timpone)	n.d.	n.d.
17	58	Stromboli (Scari)	(1) Violent explosion, ash column upwards; (2) Pyroclastic flow towards Sciara del Fuoco; (3) Ash/lapilli fall at Ginostra.	1 casualty; Wildfires on vegetated areas at Ginostra; Ash/lapilli accumulation on the roofs (obstruction of rainwater harvest cisterns and dirty water) at Ginostra.
18	70	Ginostra	(1) Explosion, ash column upwards; (2) Pyroclastic flow towards Sciara del Fuoco; (3) Impact of pyroclastic flow with the sea surface, grey cloud upwards, wildfires at Punta Corvi; (4) Ash/lapilli fall at Ginostra.	Wildfires on vegetated areas at Ginostra; Ash/lapilli accumulation on the roofs (obstruction of rainwater harvest cisterns and dirty water) at Ginostra; Damages to the canopies at Ginostra.

Table A2. *Cont.*

3 July 2019 Explosion				
19	≈75	Ginostra	(1) Explosion, ash column upwards; (2) Pyroclastic flow towards Sciara del Fuoco; (3) Ash/lapilli fall at Ginostra.	1 casualty; Wildfires on vegetated areas at Ginostra; Ash/lapilli accumulation on the roofs (obstruction of rainwater harvest cisterns and dirty water) at Ginostra; Damages to the canopies at Ginostra; Damages to the photovoltaic panels of private properties at Ginostra.
20	≈75	Ginostra	(1) Violent explosion, ash column upwards; (2) Pyroclastic flow toward Sciara del Fuoco; (3) Grey cloud upwards, wildfires at Timpone; (4) Ash/lapilli fall at Ginostra.	1 casualty; Wildfires on vegetated areas at Ginostra; Ash/lapilli accumulation on the roofs (obstruction of rainwater harvest cisterns and dirty water) at Ginostra. Damages to the canopies at Ginostra; Damages to the adjacent area of the photovoltaic power station at Ginostra.

Appendix C

Table A3. Summary of semi-structured interviews to the inhabitants of Stromboli island, after the 28 August 2019 explosion.

28 August 2019				
Interviewees	*Age*	*Location (during the event)*	*Event description*	*Damages description*
1	26	Stromboli (San Vincenzo)	n.d.	Wildfires on vegetated areas at Stromboli; Ash/lapilli accumulation on the roofs (obstruction of rainwater harvest cisterns and dirty water) at Stromboli.
2	46	Stromboli (San Vincenzo)	(1) Violent explosion, ash column upwards; (2) Ash/lapilli fall at Stromboli.	Ash/lapilli accumulation on the roofs (obstruction of rainwater harvest cisterns and dirty water) at Stromboli.
3	49	Stromboli (San Vincenzo)	n.d.	Ash/lapilli accumulation on the roofs (obstruction of rainwater harvest cisterns and dirty water) at Stromboli.
4	≈75	Stromboli (San Vincenzo)	(1) Violent explosion, ash column upwards; (2) Ash/lapilli fall at Stromboli.	Ash/lapilli accumulation on the roofs (obstruction of rainwater harvest cisterns and dirty water) at Stromboli.
5	68	Stromboli (San Vincenzo)	(1) Violent explosion, ash column upwards; (2) Ash/lapilli fall at Stromboli.	Ash/lapilli accumulation on the roofs (obstruction of rainwater harvest cisterns and dirty water) at Stromboli.
6	51	(Stromboli (Pizzillo)	(1) Violent explosion, ash column upwards; (2) Lava flows; (3) Ash/lapilli fall at Stromboli.	Ash/lapilli accumulation on the roofs (obstruction of rainwater harvest cisterns and dirty water) at Stromboli.
7	65	Stromboli (at sea)	n.d.	n.d.
8	58	Stromboli (San Vincenzo)	n.d.	n.d.
9	28	n.d.	(1) Explosion, ash column upwards; (2) Lava overflows.	Ash/lapilli accumulation on the roofs (obstruction of rainwater harvest cisterns and dirty water) at Stromboli.
10	46	n.d.	(1) Violent explosion, ash column upwards; (2) Ash/lapilli fall at Stromboli.	Ash/lapilli accumulation on the roofs (obstruction of rainwater harvest cisterns and dirty water) at Stromboli.
11	67	Stromboli (Scari)	(1) Explosion, ash column upwards; (2) Ash/lapilli fall at Stromboli.	Ash/lapilli accumulation on the roofs (obstruction of rainwater harvest cisterns and dirty water) at Stromboli.
12	60	Stromboli (Scari)	n.d.	n.d.
13	≈75	Stromboli (Scari)	(1) Violent explosion, ash column upwards; (2) Lava flows; (3) Ash/lapilli fall at Stromboli.	Wildfires on vegetated areas at Stromboli; Ash/lapilli accumulation on the roofs (obstruction of rainwater harvest cisterns and dirty water) at Stromboli.

Table A3. *Cont.*

			28 August 2019	
14	72	n.d.	(1) Explosion, ash column upwards; (2) Ash/lapilli fall at Stromboli.	Wildfires on vegetated areas at Stromboli; Ash/lapilli accumulation on the roofs (obstruction of rainwater harvest cisterns and dirty water) at Stromboli.
15	24	Stromboli (Scari)	n.d.	n.d.
16	76	Stromboli (Timpone)	n.d.	n.d.
17	58	Stromboli (Scari)	(1) Explosion, ash column upwards; (2) Ash/lapilli fall at Stromboli.	Wildfires on vegetated areas at Stromboli; Ash/lapilli accumulation on the roofs (obstruction of rainwater harvest cisterns and dirty water) at Stromboli.
18	70	Ginostra	n.d.	n.d.
19	≈75	Ginostra	n.d.	n.d.
20	≈75	Ginostra	n.d.	n.d.

References

1. Pierson, T.C.; Major, J.J. Hydrogeomorphic effects of explosive volcanic eruptions on drainage basins. *Annu. Rev. Earth Planet. Sci.* **2014**, *42*, 469–507. [CrossRef]
2. Gomez, C. Digital photogrammetry and GIS-based analysis of the bio-geomorphological evolution of Sakurajima Volcano, diachronic analysis from 1947 to 2006. *J. Volcanol. Geotherm. Res.* **2014**, *280*, 1–13. [CrossRef]
3. Barberi, F.; Rosi, M.; Sodi, A. Volcanic hazard assessment at Stromboli based on review of historical data. *Acta Vulcanol.* **1993**, *3*, 173–187.
4. Blackburn, E.A.; Wilson, L.; Sparks, R.J. Mechanisms and dynamics of strombolian activity. *J. Geol. Soc.* **1976**, *132*, 429–440. [CrossRef]
5. Calvari, S.; Bonaccorso, A.; Madonia, P.; Neri, M.; Liuzzo, M.; Salerno, G.G.; Behncke, B.; Caltabiano, T.; Cristaldi, A.; Giuffrida, G.; et al. Major eruptive style changes induced by structural modifications of a shallow conduit system: The 2007–2012 Stromboli case. *Bull. Volcanol.* **2014**, *76*, 841. [CrossRef]
6. Calvari, S.; Intrieri, E.; Di Traglia, F.; Bonaccorso, A.; Casagli, N.; Cristaldi, A. Monitoring crater-wall collapse at active volcanoes: A study of the 12 January 2013 event at Stromboli. *Bull. Volcanol.* **2016**, *78*, 39. [CrossRef]
7. Di Traglia, F.; Calvari, S.; D'Auria, L.; Nolesini, T.; Bonaccorso, A.; Fornaciai, A.; Esposito, A.; Cristaldi, A.; Favalli, M.; Casagli, N. The 2014 Effusive Eruption at Stromboli: New Insights from In Situ and Remote-Sensing Measurements. *Remote Sens.* **2018**, *10*, 2035. [CrossRef]
8. Rosi, M.; Pistolesi, M.; Bertagnini, A.; Landi, P.; Pompilio, M.; Di Roberto, A. Stromboli volcano, Aeolian Islands (Italy): Present eruptive activity and hazards. *Geol. Soc. Lond. Mem.* **2013**, *37*, 473–490. [CrossRef]
9. Plank, S.; Marchese, F.; Filizzola, C.; Pergola, N.; Neri, M.; Nolde, M.; Martinis, S. The July/August 2019 Lava Flows at the Sciara del Fuoco, Stromboli–Analysis from Multi-Sensor Infrared Satellite Imagery. *Remote Sens.* **2019**, *11*, 2879. [CrossRef]
10. Lutes, D.C.; Keane, R.E.; Caratti, J.F.; Key, C.H.; Benson, N.C.; Sutherland, S.; Gangi, L.J. *FIREMON: Fire Effects Monitoring and Inventory System*; General Technical Report RMRS-GTR-164; US Department of Agriculture, Forest Service, Rocky Mountain Research Station: Fort Collins, CO, USA, 2006; pp. 1–164.
11. Keeley, J.E. Fire intensity, fire severity and burn severity: A brief review and suggested usage. *Int. J. Widland Fire* **2009**, *18*, 116–126. [CrossRef]
12. Parks, S.A.; Dillon, G.K.; Miller, C. A new metric for quantifying burn severity: The relativized burn ratio. *Remote Sens.* **2014**, *6*, 1827–1844. [CrossRef]
13. Sobrino, J.A.; Llorens, R.; Fernández, C.; Fernández-Alonso, J.M.; Vega, J.A. Relationship between Soil Burn Severity in Forest Fires Measured In Situ and through Spectral Indices of Remote Detection. *Forests* **2019**, *10*, 457. [CrossRef]
14. Babu, K.V.; Roy, A.; Aggarwal, R. Mapping of Forest Fire Burned Severity Using the Sentinel Datasets. *ISPRS Int. Arch. Photogramm. Remote Sens. Spat. Inf. Sci.* **2018**, *425*, 469–474. [CrossRef]

15. Teodoro, A.; Amaral, A. A Statistical and Spatial Analysis of Portuguese Forest Fires in Summer 2016 Considering Landsat 8 and Sentinel 2A Data. *Environments* **2019**, *6*, 36. [CrossRef]
16. Pepe, M.; Parente, C. Burned area recognition by change detection analysis using images derived from Sentinel-2 satellite: The case study of Sorrento Peninsula, Italy. *J. Appl. Eng. Sci.* **2018**, *16*, 225–232. [CrossRef]
17. Fisher, P.F.; Comber, A.J.; Wadsworth, R. Land use and land cover: Contradiction or complement. In *Re-Presenting GIS*; Fisher, P., Unwin, D., Eds.; John Wiley & Sons: Hoboken, NJ, USA, 2005; pp. 1–293.
18. Di Traglia, F.; Fornaciai, A.; Favalli, M.; Nolesini, T.; Casagli, N. Catching Geomorphological Response to Volcanic Activity on Steep Slope Volcanoes Using Multi-Platform Remote Sensing. *Remote Sens.* **2020**, *12*, 438. [CrossRef]
19. Tinti, S.; Mannucci, A.; Pagnoni, G.; Armigliato, A.; Zaniboni, F. The 30 December 2002 landslide-induced tsunamis in Stromboli: Sequence of the events reconstructed from the eyewitness accounts. *Nat. Hazards Earth Syst. Sci.* **2005**, *5*, 763–775. [CrossRef]
20. Alleruzzo Di Maggio, M.T.; Formica, M.T.; Fornaro, A.; Gambino, J.C.; Pecora, A. *La Casa Rurale Nella Sicilia Orientale*, 2nd ed.; Leo, S., Ed.; Olschki Editore: Firenze, Italy, 2012.
21. Lavigne, F.; Thouret, J.C. Sediment transportation and deposition by rain-triggered lahars at Merapi Volcano, Central Java, Indonesia. *Geomorphology* **2003**, *49*, 45–69. [CrossRef]
22. Gran, K.B.; Montgomery, D.R. Spatial and temporal patterns in fluvial recovery following volcanic eruptions: Channel response to basin-wide sediment loading at Mount Pinatubo, Philippines. *Geol. Soc. Am. Bull.* **2005**, *17*, 195–211. [CrossRef]
23. Major, J.J.; Mark, L.E. Peak flow responses to landscape disturbances caused by the cataclysmic 1980 eruption of Mount St. Helens, Washington. *Geol. Soc. Am. Bull.* **2006**, *118*, 938–958. [CrossRef]
24. Pierson, T.C.; Pringle, P.T.; Cameron, K.A. Magnitude and timing of downstream channel aggradation and degradation in response to a dome-building eruption at Mount Hood, Oregon. *GSA Bull.* **2011**, *123*, 3–20. [CrossRef]
25. Wadge, G.; Cole, P.; Stinton, A.; Komorowski, J.C.; Stewart, R.; Toombs, A.C.; Legendre, Y. Rapid topographic change measured by high-resolution satellite radar at Soufriere Hills Volcano, Montserrat, 2008–2010. *J. Volcanol. Geotherm. Res.* **2011**, *199*, 142–152. [CrossRef]
26. Kassouk, Z.; Thouret, J.C.; Gupta, A.; Solikhin, A.; Liew, S.C. Object-oriented classification of a high-spatial resolution SPOT5 image for mapping geology and landforms of active volcanoes: Semeru case study, Indonesia. *Geomorphology* **2014**, *221*, 18–33. [CrossRef]
27. Thouret, J.C.; Oehler, J.F.; Gupta, A.; Solikhin, A.; Procter, J.N. Erosion and aggradation on persistently active volcanoes—A case study from Semeru Volcano, Indonesia. *Bull. Volcanol.* **2014**, *76*, 857. [CrossRef]
28. Biass, S.; Falcone, J.L.; Bonadonna, C.; Di Traglia, F.; Pistolesi, M.; Rosi, M.; Lestuzzi, P. Great Balls of Fire: A probabilistic approach to quantify the hazard related to ballistics—A case study at La Fossa volcano, Vulcano Island, Italy. *J. Volcanol. Geotherm. Res.* **2016**, *325*, 1–14. [CrossRef]
29. Biass, S.; Bonadonna, C.; Di Traglia, F.; Pistolesi, M.; Rosi, M.; Lestuzzi, P. Probabilistic evaluation of the physical impact of future tephra fallout events for the Island of Vulcano, Italy. *Bull. Volcanol.* **2016**, *78*, 37. [CrossRef]
30. Calvari, S.; Spampinato, L.; Lodato, L. The 5 April 2003 vulcanian paroxysmal explosion at Stromboli volcano (Italy) from field observations and thermal data. *J. Volcanol. Geotherm. Res.* **2006**, *149*, 160–175. [CrossRef]
31. Salvatici, T.; Di Roberto, A.; Di Traglia, F.; Bisson, M.; Morelli, S.; Fidolini, F.; Bertagnini, A.; Pompilio, M.; Hungr, O.; Casagli, N. From hot rocks to glowing avalanches: Numerical modelling of gravity-induced pyroclastic density currents and hazard maps at the Stromboli Volcano (Italy). *Geomorphology* **2016**, *273*, 93–106. [CrossRef]
32. Magnaghi, A. *Il Progetto Locale*, 1st ed.; Bollati Boringhieri: Torino, Italia, 2000.
33. Magnaghi, A. *Rappresentare i Luoghi: Metodi e Tecniche*, 1st ed.; Alinea Editrice: Firenze, Italia, 2001.
34. Moreira, F.; Viedma, O.; Arianoutsou, M.; Curt, T.; Koutsias, N.; Rigolot, E.; Barbati, A.; Corona, P.; Vaz, P.; Xanthopoulos, G.; et al. Landscape—Wildfire interactions in southern urope: Implication for landscape managment. *J. Environ. Manag.* **2011**, *92*, 2389–2402. [CrossRef]
35. Vos, W. Recent landscape transformation in the Tuscan Apennines caused by changing land use. *Landsc. Urban Plann.* **1993**, *24*, 63–68. [CrossRef]
36. Nagaike, T.; Kamitani, T. Factors affecting changes in a landscape structure dominated by both primary and coppice forests in the Fagus crenata forest region on central Japan. *J. For. Res.* **1997**, *2*, 193–198. [CrossRef]

37. Luque, S.S. The challenge to manage the biological integrity of nature reserves: A landscape ecology perspective. *Int. J. Remote Sens.* **2000**, *21*, 2613–2643. [CrossRef]
38. Blasi, C.; Milone, M.; Guida, D.; De Filippo, G.; Di Gennaro, A.; La Valva, V.; Nicoletti, D. Ecologia del paesaggio e qualità ambientale del Parco Nazionale del Cilento e Vallo di Diano. *Doc. Territ.* **2001**, *46*, 20–30.
39. Blasi, C.; Fortini, P.; Carranza, M.L.; Frondoni, R.; Ricotta, C. Analisi della diversità del paesaggio vegetale e dei processi di recupero nella media valle dell'Aniene (Appennino centrale, Lazio). *Fitosociologia* **2001**, *38*, 3–11.
40. Blasi, C.; Smiraglia, D.; Carranza, M.L. Analisi multitemporale del paesaggio e classificazione gerarchica del territorio: Il caso dei Monti Lepini (Italia centrale). *Inf. Bot. Ital.* **2003**, *35*, 31–40.
41. Rothermel, R. *How to Predict the Spread and Intensity of Forest and Range Fires*; General Technical Report INT-143; USDA, Forest Service, Intermountain Forest and Range Experiment Station: Ogden, UT, USA, 1983.
42. Fernandes, P.; Botelho, H. A review of prescribed burning effectiveness in fire hazard reduction. *Int. J. Wildland Fire* **2003**, *12*, 117–128. [CrossRef]
43. Fernandes, P. Forest fires in Galicia (Spain): The outcome of unbalanced fire management. *J. For. Econ.* **2008**, *14*, 155–157. [CrossRef]
44. Moreira, F.; Vaz, P.; Catry, F.; Silva, J.S. Regional variations in wildfire susceptibility of land-cover types in Portugal: Implications for landscape management to minimize fire hazard. *Int. J. Wildland Fire* **2009**, *18*, 563–574. [CrossRef]